Inorg. Chem. **2005**, *44*, 9895–9901

Synthesis and Growth Mechanisms of One-Dimensional Strontium Hydroxyapatite Nanostructures

Tae-Gon Kim* and Byungwoo Park*

School of Materials Science and Engineering, Seoul National University, Seoul, Korea

Received June 21, 2005

Strontium hydroxyapatite (SrHAp) nanowires with an aspect ratio of several hundreds were synthesized by controlling the growth conditions during a hydrothermal process. In the strontium phosphate system, it was found that the phase evolution changed with pH and that the aspect ratio of SrHAp was affected by the phases present before heating. Since the conditions for SrHAp nucleation prohibits one-dimensional growth, it was impossible to grow large-scale SrHAp nanowires using routine hydrothermal methods. Through thermodynamic considerations, the mechanisms of nanowire formation appear to involve the rapid release of the stored chemical potential in a metastable phase, which promotes the anisotropic growth of the most stable SrHAp nanostructures. Thereby, the conditions for both the nucleation of the SrHAp phase and the anisotropic growth were determined simultaneously, and considerable quantities of SrHAp nanowires were synthesized.

Introduction

One-dimensional nanostructures have attracted a great deal of interest because of their novel physical and chemical properties resulting from size and dimensionality. In addition, they have potential applications as interconnections in nanoelectronics, single-electron transistors, light-emitting diodes, gas and chemical sensors, optical detectors, lasers, etc.[1−9] Many synthetic strategies have been developed to produce these nanostructures, such as the vapor−liquid−solid process, template-directed growth, kinetic control provided by a capping reagent, maximizing the intrinsically anisotropic crystal structures, etc.[2,3,10−21] Among them, methods using anisotropic surface energy are suitable for the facile, inexpensive, and organic or catalyst contamination-free production of nanostructures.

Apatites are well-known biocompatible materials, which also have many other novel properties, such as the dehydrogenation of hydrocarbons and alcohols (catalyst), the separation of protein and nucleic acid (liquid-chromatographic columns), photoluminescence (lighting materials), the removal of heavy-metal ions (powder carriers), sensing various gases or humidity (chemical sensors), O^{2-}/OH^{-}/proton conduction (ion conductors), etc.[22−27] Many of these properties are affected by the size and morphology of the individual particles. In particular, the enhanced mechanical

* To whom correspondence should be addressed. E-mail: stylers2@snu.ac.kr (T.-G.K.); byungwoo@snu.ac.kr (B.P.).

(1) Sun, Y.; Gates, B.; Mayer, B.; Xia, Y. *Nano Lett.* **2002**, *2*, 165.
(2) Gudikson, M. S.; Lauhon, L. J.; Wang, J.; Smith, D. C.; Lieber, C. M. *Nature* **2002**, *415*, 617.
(3) Lauhon, L. J.; Gudikson, M. S.; Wang, J.; Smith, D. C.; Lieber, C. M. *Nature* **2002**, *420*, 57.
(4) Yan, H.; He, R.; Johnson, J.; Law, M.; Saykally, R. J.; Yang, P. *J. Am. Chem. Soc.* **2003**, *125*, 4728.
(5) Meyssamy, H.; Riwotzki, K.; Kornowski, A.; Naused, S.; Haase, M. *Adv. Mater.* **1999**, *11*, 840.
(6) Wang, Y.; Jiang, X.; Xia, Y. *J. Am. Chem. Soc.* **2003**, *125*, 16176.
(7) Klimov, V. I.; Mikailovsky, A. A.; Xu, S.; Malko, A.; Hollingsworth, J. A.; Leaterdale, C. A.; Eisler, H. J.; Bawendi, M. G. *Science* **2000**, *314*, 290.
(8) Kim, E.; Son, D.; Kim, T.-G.; Cho, J.; Park, B.; Ryu, K.-S.; Chang, S.-H. *Angew. Chem. Int. Ed.* **2004**, *43*, 5987.
(9) Cho, J.; Kim, Y.-W.; Kim, B.; Lee, J.-G.; Park, B. *Angew. Chem. Int. Ed.* **2003**, *42*, 1618.
(10) Hulteen, J. C.; Martin, C. R. *J. Mater. Chem.* **1997**, *7*, 1075.
(11) Urban, J. J.; Yun, W. S.; Gu, Q.; Park, H. *J. Am. Chem. Soc.* **2002**, *124*, 1186.
(12) Peng, Z. A.; Peng, X. *J. Am. Chem. Soc.* **2001**, *123*, 1389.
(13) Peng, X. *Adv. Mater.* **2003**, *15*, 459.
(14) Yu, S.-H.; Liu, B.; Mo, M.-S.; Huang, J.-H.; Liu, X.-M.; Qian, Y.-T. *Adv. Funct. Mater.* **2003**, *13*, 639.
(15) Gates, B.; Ying, Y.; Xia, Y. *J. Am. Chem. Soc.* **2000**, *122*, 12582.
(16) Mayer, B.; Xia, Y. *Adv. Mater.* **2002**, *14*, 279.
(17) Xie, J. L. Y.; Xu, F.; Zhu, L. *J. Mater. Chem.* **2002**, *12*, 2755.
(18) Fang, Y.-P.; Xu, A.-W.; Song, R.-Q.; Zhang, H.-X.; You, L.-P.; Yu, J. C.; Liu, H.-Q. *J. Am. Chem. Soc.* **2003**, *125*, 16025.
(19) Wang, X.; Li, Y. *Angew. Chem., Int. Ed.* **2002**, *41*, 4790.
(20) Xu, A.-W.; Fang, Y.-P.; You, L.-P.; Liu, H.-Q. *J. Am. Chem. Soc.* **2003**, *125*, 1494.
(21) Xia, Y.; Yang, P.; Sun, Y.; Wu, Y.; Mayer, B.; Gates, B.; Yin, Y.; Kim, F.; Yan, H. *Adv. Mater.* **2003**, *15*, 353.
(22) Sugiyama, S.; Minami, T.; Hayashi, H.; Tanaka, M.; Moffat, J. B. *J. Solid State Chem.* **1996**, *126*, 242.
(23) Matsumura, Y.; Sugiyama, S.; Hayashi, H.; Shigemota, N.; Saitoh, K.; Moffat, J. B. *J. Mol. Catal.* **1994**, *92*, 81.
(24) Kawasaki, T. *J. Chromatogr.* **1978**, *151*, 95.
(25) Ramesh, R.; Jagannathan, R. *J. Phys. Chem. B* **2000**, *104*, 8351.
(26) Takeda, H.; Seki, Y.; Nakamura, S.; Yamashita, K. *J. Mater. Chem.* **2002**, *12*, 2490.
(27) Adachi, G.; Imanaka, N.; Tamura, S. *Chem. Rev.* **2002**, *102*, 2405.

10.1021/ic051013m CCC: $30.25
Published on Web 11/09/2005

properties and bioactivities on the nanoscale can be expected for clinical applications.[28,29] Thus far, a large number of studies have focused only on growing large single crystals, controlling the stoichiometry, kinetics and thermodynamics of dissolution, and nucleation of the apatite materials.[30−35] Some studies dealing with the morphology of hydroxyapatite reported the synthesis of nanorods or nanowires with the assistance of hazardous organic templates or surfactants, which make it difficult to directly apply the surfaces of apatites to biological systems.[36−38] Therefore, it is preferable for nanostructured apatites to be synthesized without any assistance from organic substances.

In this study, the nucleation and growth mechanism of strontium hydroxyapatite ($Sr_5(PO_4)_3OH$, SrHAp) was examined. Large amounts of nanowires with a high aspect ratio, which are rarely acquired by a routine hydrothermal method, were synthesized in a ligand-, surfactant-, or polymer-free system. The effect of metastable-precursor particles was closely examined for the one-dimensional anisotropic growth, which had not been significantly considered in the open literature.

Experimental Section

Distilled−deionized water (DDW) with a pH 7.5, 9.5, 10.3, 10.5, and 11.2 that was controlled with an ammonia solution (NH_4OH) was used. Analytical grade $Sr(NO_3)_2$ (0.18 g) and $(NH_4)_2HPO_4$ (0.07 g) powders were dissolved in 50 mL of the pH-controlled water, and the strontium and phosphate source solutions were mixed and magnetically stirred for 10 min at room temperature, resulting in the formation of a suspension containing white precipitates. The resulting suspension was poured into a Teflon-lined stainless steel autoclave, which was maintained at 180 °C in a temperature-controlled oven for 10 h. The reaction was then quenched by cooling the suspension to room temperature. In the final suspension, clear solutions were extracted for compositional analysis by centrifugation, and the precipitates were washed with DDW and dried at 80 °C in air for 5 h.

To acquire the SrHAp nanowires as a major phase, two strontium and phosphate source solutions were prepared using the water at pHs of 7.5 and 10.5, and they were mixed at room temperature. The nanoparticles that were separated by centrifugation from the suspension made at pH 7.5 were dispersed in the clear solution that had been filtered from the colloid synthesized at pH 10.5. The newly mixed suspension was poured into a Teflon-lined stainless steel autoclave and heated to 180 °C in an oven for 10 h. The reaction was then quenched by cooling the suspension to room temperature. The resulting product was filtered, washed with DDW, and dried at 80 °C in air for 5 h.

The phase and morphology of the obtained samples were characterized by X-ray diffraction (XRD, M18XHF−SRA: MAC science) using Cu Kα radiation ($\lambda = 0.15418$ nm), field-emission scanning electron microscopy (FE-SEM, JSM-6330F: JEOL) at an operating voltage of 20 kV, and transmission electron microscopy (TEM, JEM-200CX: JEOL) operating at 200 keV. The concentrations and pH of the solutions were measured by inductive-coupled plasma atomic-emission spectroscopy (ICP-AES, ICPS-7500: SHIMADZU) and a pH meter (inoLab pH 720: WTW GmbH), respectively. The ionic strength of the solution was determined by conductivity measurements (Orion 115Aplus: Thermo Electron Co.) through the reported relation $I(\text{mM}) = 0.0021 + 0.0148\sigma(\mu\text{S/cm})$, where σ is the ionic conductivity in water at 25 °C.[39] The unit-cell structure was visualized using ATOMS (version 5.1) software.

Table 1. Changes in the pH of the Solution or Suspension in Each Experimental Step

initial pH	pH after dissolving $(NH_4)_2HPO_4$	pH after mixing the sources at 25 °C	pH after heating at 180 °C
7.5	8.1	6.6	5.7
9.5	8.2	6.7	6.4
10.3	8.5	7.1	7.1
10.5	8.7	9.5	9.0
11.2	10.1	10.2	10.2

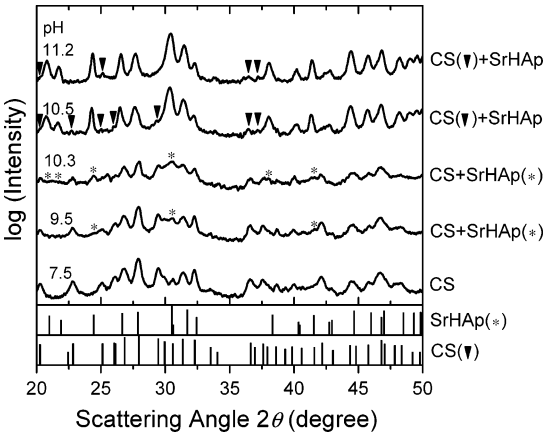

Figure 1. Phase change of strontium phosphate as a function of pH after the source solutions were mixed at 25 °C. The pH values were 7.5, 9.5, 10.3, 10.5, and 11.2 from the bottom to top. The ideal peak positions and intensities are marked for SrHAp (JCPDS 33-1348) and CS (ref 40).

Results

Table 1 shows the pH changes in the solution at each experimental step. The pH after the $Sr(NO_3)_2$ dissolved was not included because there was little change. Since hydrogenphosphate ions buffered the pH via the association and dissociation of hydrogen ions, the pH intervals became closer after the $(NH_4)_2HPO_4$ was dissolved. Overall, the pH of the suspensions gradually decreased with time. For a simple indication, the initially controlled pH values (i.e., pH 7.5, 9.5, 10.3, 10.5, and 11.2) are used as representatives among the four steps of pH (Table 1) in this article. In some cases, the actual (and physically meaningful) pH is reported. Figure 1 shows the XRD patterns of the various strontium phosphates that precipitated after the source solutions were mixed at 25 °C. The most soluble phase, Collin's salt ($Sr_6H_3(PO_4)_5 \cdot 2H_2O$, CS), was fully precipitated at an initial pH of 7.5.[41,42]

(28) Mann, S.; Ozin, G. A. *Nature* **1996**, *382*, 313.
(29) Ahn, E. S.; Gleason, N. J.; Nakahira, A.; Ying, J. Y. *Nano Lett.* **2001**, *1*, 149.
(30) Kirn, J. F.; Leidheiser, H., Jr. *J. Cryst. Growth* **1968**, *2*, 111.
(31) Jullmann, H.; Masebach, R. *Z. Naturforsch. B* **1966**, *21*, 493.
(32) Christoffersen, J.; Christoffersen, M. R.; Kolthoff, N.; Bärenholdt, O. *Bone* **1997**, *20*, 47.
(33) Rodríquez-Lorenzo, L. M.; Vallet-Regí, M. *Chem. Mater.* **2000**, *12*, 2460.
(34) Tang, R.; Nancollas, G. H.; Orme, C. A. *J. Am. Chem. Soc.* **2001**, *123*, 5437.
(35) van Kemenade, M. J. J. M.; de Bruin, P. L. *J. Colloid Interface Sci.* **1987**, *118*, 564.
(36) Cao, M.; Wang, Y.; Guo, C.; Qi, Y.; Hu, Q. *Langmuir* **2004**, *21*, 4784.
(37) Liu, Y. K.; Wang, W. Z.; Zhan, Y. J.; Zheng, C. L.; Wang, G. H. *Mater. Lett.* **2002**, *56*, 496.
(38) Yan, L.; Li, Y. D.; Deng, Z. X.; Zhuang, J.; Sun, X. M. *Int. J. Inorg. Mater.* **2001**, *3*, 633.

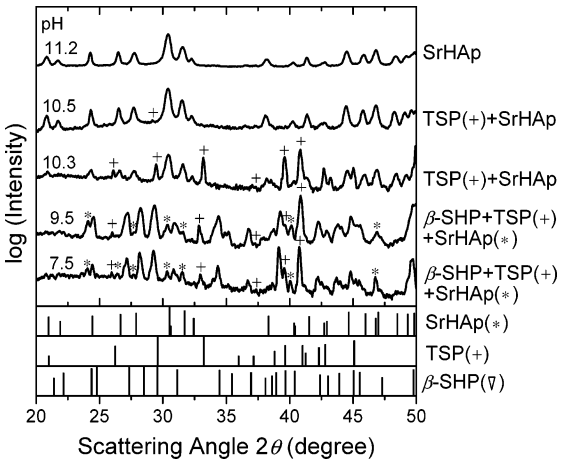

Figure 2. Phase change in strontium phosphate as a function of pH after the suspension was heated to 180 °C. The pH values are 7.5, 9.5, 10.3, 10.5, and 11.2 from bottom to top. The ideal peak positions and intensities are marked for SrHAp, TSP (JCPDS 24-1008), and β-SHP (ref 43).

A stable SrHAp phase began to form at pH 9.5 and was approximately half that formed at pH 10.3. The SrHAp phase with a negligible fraction of the CS phase was synthesized at pH 10.5 and 11.2. Figure 2 shows the phase changes in the strontium phosphate, which was precipitated by heating the suspension containing the precursor particles at 180 °C at various pHs. Tristrontium phosphate ($Sr_3(PO_4)_2$, TSP), β-strontium hydrogen phosphate ($SrHPO_4$, β-SHP), and a fraction of SrHAp were obtained from the suspension produced at pH 7.5 and 9.5. These phases are believed to have transformed from CS during heating. The SrHAp phase, which was fully synthesized in the pH 10.5 and 11.2 solutions, was quite stable after heating. As a transition stage, a mixed phase of SrHAp and TSP was formed at pH 10.3. By considering the increase in the relative fraction of SrHAp before and after heating, we suggest that SrHAp at pH 10.3 consists of an originally existing SrHAp and the SrHAp phase transformed from CS.

The morphological change in the phosphates was investigated as a function of pH using SEM and TEM, as shown in Figure 3. The striped arrow shows the increase in the pH. The CS and SrHAp synthesized before heating had "plate-like" and "rice-shaped" morphologies, respectively (the left column in Figure 3). After the suspension was heated at 180 °C, small quantities of SrHAp nanowires with aspect ratios of several hundreds (average width of ~30 nm and lengths of up to 3 − 7 μm) were observed at pHs of 7.5 and 9.5. The major phases, TSP and β-SHP, were easily observed with TEM, as shown in Figure 3. TSP shows very large single-crystalline particles with a diameters of several tens of micrometers, and β-SHP shows '"flake- or platelike" particles with widths of several hundred nanometers at pHs of 7.5 and 9.5. The CS, SrHAp, and β-SHP phases were identified from their electron diffraction patterns. The TSP phase was indirectly confirmed as the sole unidentified phase in the phase mixture determined by XRD because the TSP was too thick for the electron beam to penetrate the sample. In the suspension at pH 10.3, all the SrHAp particles (after heating) had a one-dimensional morphology with a bimodal distribution of aspect ratios as ~100 (~40 nm × ~4 μm)

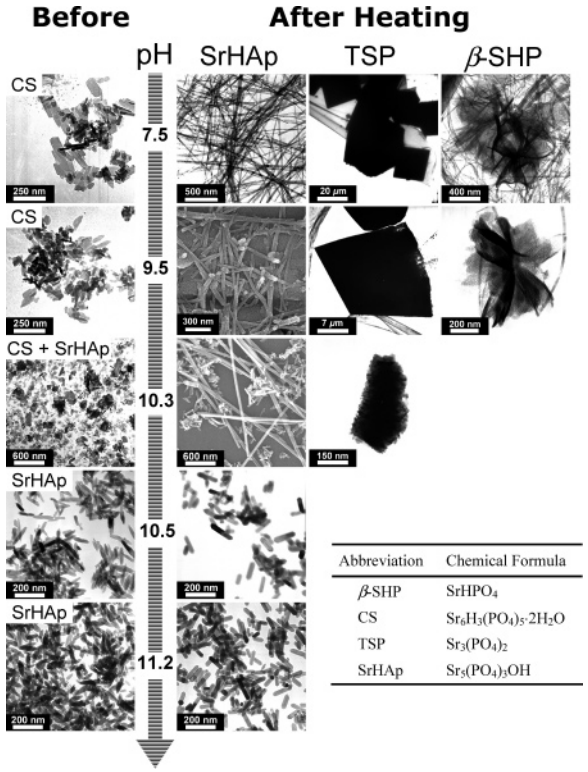

Abbreviation	Chemical Formula
β-SHP	$SrHPO_4$
CS	$Sr_6H_3(PO_4)_5 \cdot 2H_2O$
TSP	$Sr_3(PO_4)_2$
SrHAp	$Sr_5(PO_4)_3OH$

Figure 3. Morphological change in strontium phosphate as a function of the pH values of the source solutions. The abbreviations frequently used in this article are also summarized.

Table 2. SrHAp Nanoparticle Sizes Determined from the XRD Data in Figure 2 from the Scherrer Equation Using the (200), (300), (400), and (002) Diffraction Peaks

	pH 10.5	pH 11.2
width (*a* axis)	45.2 ± 12.7 nm	22.8 ± 2.8 nm
length (*c* axis)	138 ± 19 nm	186 ± 21 nm

and ~6 (~30 nm × ~200 nm). The fraction of long wires was smaller than that of the rods. In addition, small- and large-sized TSP was also found in the pH 10.3 system. The SrHAp nanostructures in the systems at pH 10.5 and 11.2 show a very similar morphology of short nanorods with an aspect ratio of only ~5 (~30 nm × ~150 nm), which is consistent with the XRD results of Figure 2 which were analyzed using the Scherrer equation (summarized in Table 2).[44] Figure 4 is a schematic diagram showing a summary of the changes in the phases before and after heating and the aspect ratio of the SrHAp nanostructures. A comparison of the phase constitution before heating (Figure 4a) with the final morphology of SrHAp (Figure 4c) shows that they are related.

Discussion

I. Phase Evolution of Strontium Phosphates. To understand the mechanism of phase evolution, we calculated solubility isotherms at 25 and 180 °C using the effective chemical reactions and their solubility products, as shown in Appendix I of the Supporting Information. In Figure 5, the solubility phase diagram is plotted alongside the product of the total strontium and phosphate activities ($(P)_{tot} \times (Sr)_{tot}$, where () denotes the activity of the component) as a function

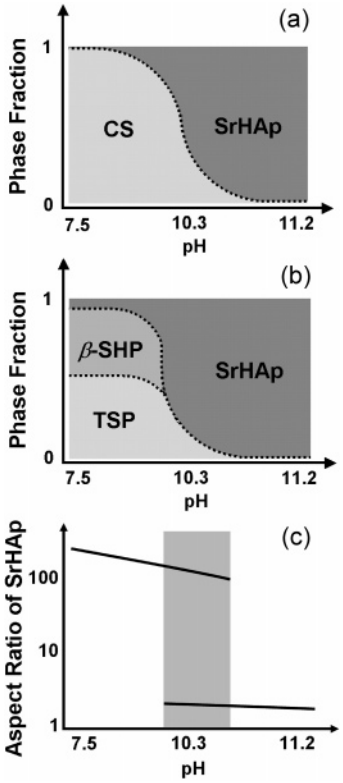

Figure 4. Schematic diagrams of the phase changes (a) before and (b) after heating, and (c) the aspect ratio of SrHAp after heating as a function of pH.

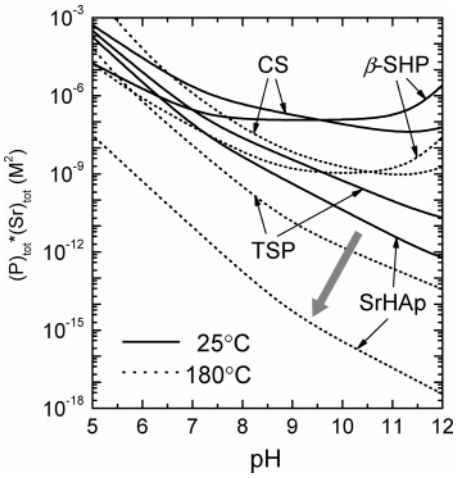

Figure 5. Calculated solubility isotherms of the Collin's salt, β-SHP, TSP, and SrHAp at 25 (solid line) and 180 °C (dotted line) as $(P)_{tot} \times (Sr)_{tot}$ with pH. $(P)_{tot} \times (Sr)_{tot}$ is the product of total phosphate and strontium activity in solution. The chosen Sr/P ratio is 1.67.

of the pH. The process used to calculate the solubility isotherms is detailed in Appendix II of the Supporting Information.

It is generally known that the order of precipitation in a system where the different phases have different solubility follows the Ostwald rule of stages.[35,42,43,45] The rule states

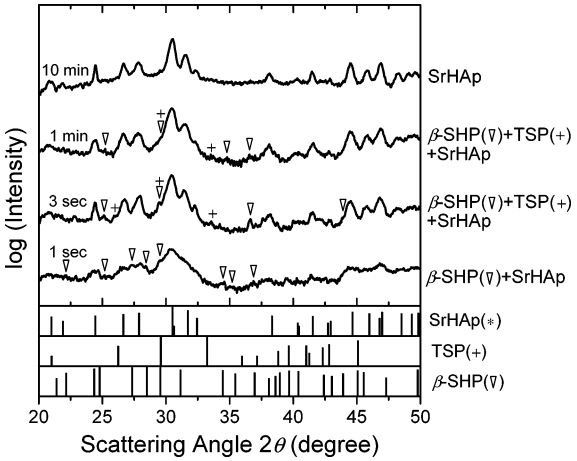

Figure 6. Phase evolution as a function of time, immediately after the source solutions were mixed at pH 10.5 at 25 °C. An equal volume of methanol was poured into the reaction bowl to rapidly quench the transformation.

that the least thermodynamically stable phase will form first, then transform into more stable phases under a given condition. Considering the solubility isotherm in Figure 5, the nucleation sequence at 25 °C should be CS, β-SHP, TSP, and SrHAp at pHs below ~9.5 and β-SHP, CS, TSP, and SrHAp at pHs above ~9.5. In the experiment, the phases that precipitated at 25 °C varied from CS to SrHAp with increasing pH. To be consistent with the rule, it should be noted that the time for the phase conversion (kinetics) depends on the pH. Indeed, the phase transformation from β-SHP to SrHAp via TSP at 25 °C was detected over a 10 min period at pH 10.5 (the real pH ranged from 8.7 to 9.5, as shown in Table 1), even though a large amount of SrHAp was produced directly in the initial period of precipitation where there was a high supersaturation (Figure 6).[35,41,42] On the other hand, the phase conversion from CS to β-SHP at pH 7.5 was detected after approximately one week at 25 °C (data not shown). As a result, the difference in the phase-conversion time causes variations in the precipitated phases with pH.

The order of phase evolution at 180 °C in the low pH solution was also consistent with the prediction of the rule of stages (CS, β-SHP, TSP, and SrHAp, or CS, TSP, β-SHP, and SrHAp at 180 °C, as shown in Figure 5). Figure 7a shows the phase change of the precipitates in the solution at pH 7.5 as a function of time at 180 °C. The β-SHP and TSP phases began to appear after 1.5 h, and their proportion gradually increased with encroaching CS in the system initially controlled as pH 7.5. After 10 h, the CS phase had disappeared completely, and the β-SHP and TSP phases occupied the majority with a small fraction of SrHAp.

II. Shape Evolution of Strontium Hydroxyapatite Nanostructures. After the solutions were heated at 180 °C,

(39) Talbot, J. D. R.; House, W. A.; Pethybridge, A. D. *Water Res.* **1990**, *24*, 1295.
(40) Collin, R. L. *J. Chem. Eng. Data* **1964**, *9*, 165.
(41) Collin, R. L. *Science* **1966**, *151*, 1386.
(42) Feenstra, T. P.; van Straten, H. A.; de Bruin, P. L. *J. Colloid Interface Sci.* **1980**, *80*, 225.
(43) Ropp, R. C.; Aia, M. A.; Hoffman, C. W. W.; Veleker, T. J.; Mooney, R. W. *Anal. Chem.* **1959**, *31*, 1163.
(44) Warren, B. E. *X-ray Diffraction*, 1st ed.; Addison-Wesley: Reading, MA, 1969.
(45) Markov, I. V. *Crystal Growth for Beginners, Fundamentals of Nucleation, Crystal Growth and Epitaxy*, 1st ed.; World Scientific Publishing Co.: River Edge, NJ, 1995.

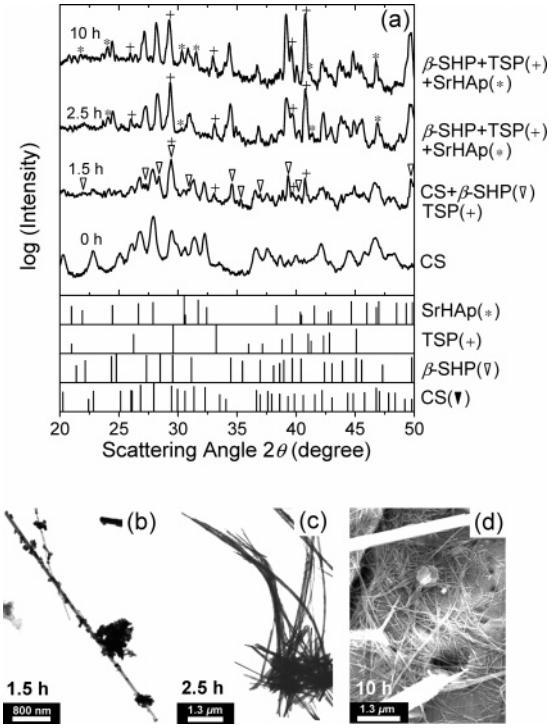

Figure 7. (a) Phase change in strontium phosphate at pH 7.5, and (b, c, and d) morphological evolution of SrHAp as a function of time at 180 °C.

the SrHAp particles which precipitated in the solutions with initial pHs of 10.5 and 11.2 at 25 °C were only trimmed from rice-shaped to round rod-shaped particles without any significant morphological change, as shown in Figure 3. Since SrHAp is the most thermodynamically stable phase, the precipitates reached an equilibrium state with the surroundings even during heating. This can be seen in Figure 5 where the activity of the total ions ($(Sr)_{tot} \times (P)_{tot}$) near the SrHAp particles is on the solubility line, which gradually decreases along the gray arrow from 25 to 180 °C. During this process, the precipitates form a thermodynamically preferred shape (without a phase change) which was predicted by the Gibbs−Curie−Wulff law through intraparticle ripening.[12,13]

On the other hand, the metastable phase formed at pH 7.5, 9.5, and 10.3 (at 25 °C) underwent a phase transformation via dissolution and reprecipitation to a more stable phase during heating at 180 °C. The difference in the thermodynamic driving force between the metastable and stable phases determines the flux of the monomers, as described in the generalized Fick's law.[46] The driving forces from β-SHP and TSP to SrHAp during the transformation were estimated to be approximately 300 and 100 kJ/mol, respectively using equations 1, 2, 9, and 10 in Appendixes II and III of the Supporting Information. Both cases were considered because it was difficult to experimentally determine if SrHAp was transformed from β-SHP or TSP at pH 7.5. Because of the release of energy from the metastable phase, the dissolved

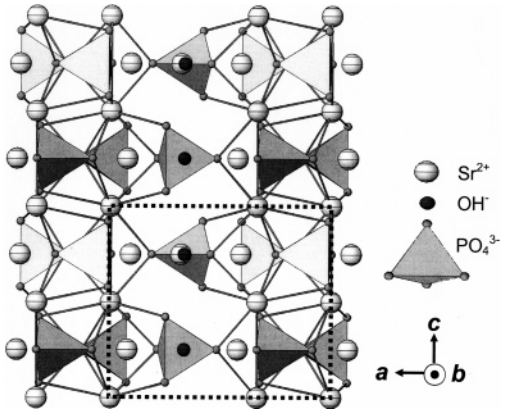

Figure 8. Crystal structure ($P6_3/m$) of SrHAp along the *c* axis.[47] The unit cell is indicated by a dotted rectangle.

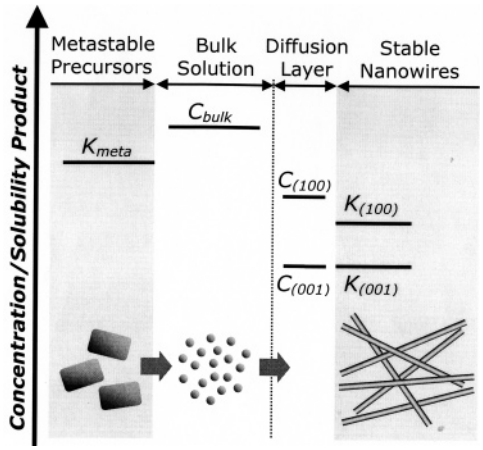

Figure 9. Suggested mechanism for the one-dimensional growth with a metastable precursor phase, where *K* is the solubility product and *C* is the concentration of monomers. The subscripts meta, bulk, (100), and (001) denote the metastable precursor phase, the bulk solution, the diffusion layer, the (100) surface of SrHAp, and the (001) surface of SrHAp, respectively.

monomers locally form high chemical-potential environments for the precipitation of SrHAp.

Peng et al. reported that the diffusion-controlled lateral growth occurs under the condition of a higher chemical potential of the monomers in the solution than that of the atoms on the unique surface of nanoparticles.[12−14] In this argument, the anisotropic reactivity of the surfaces and the high chemical-potential environment play a key role in the highly preferential growth along a specific direction.[12−21] In the crystal structure of SrHAp, as shown in Figure 8, the columns were built up of Sr^{2+} ions coordinated by nine oxygen atoms in PO_4^{3+} tetrahedra ions extending along the *c* axis making chainlike building blocks.[47,48] This atomic structure makes the interfacial free energy of the (001) plane perpendicular to the *c* axis much higher than those of the other surfaces or anisotropic structures.[48] Therefore, SrHAp grew with an anisotropic crystal structure as one-dimensional nanowires in the high chemical-potential surroundings, which were created by the release of stored energy in the prenucleated metastable phase during heating at the appropriate temperature. Figure 9 shows a schematic diagram of the

(46) Christian, J. W. *The Theory of Transformations in Metals and Alloys, An Advanced Textbook in Physical Metallurgy, Part I. Equllibrium and General Kinetics*, 2nd ed.; Pergamon Press Ltd.: Elmsford, NY, 1975.

(47) Sudarsan, K.; Young, R. A. *Acta Crystallogr. B* **1972**, *28*, 3668.

(48) Elliott, J. C. *Structure and Chemistry of the Apatites and Other Calcium Orthophosphates*; Elsevier: New York, 1994.

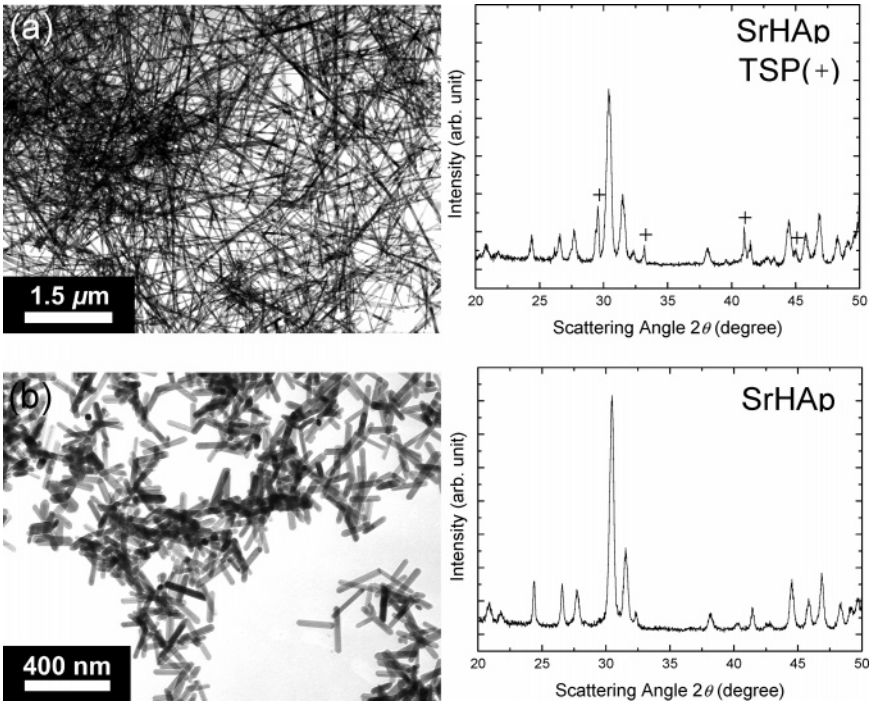

Figure 10. Morphologies and phases of the SrHAp acquired (a) by mixing the sources at pH 7.5 at 25 °C and heating the precipitates in pH 10.5 solution at 180 °C and (b) by mixing and heating the suspension in the pH 10.5 solution.

mechanisms involved. The difference in solubility between the stable and metastable phases contributes to the fundamental driving forces for this reaction. The vertically dotted line shows that the process is controlled by the diffusion of monomers between the bulk solution and the diffusion layer. Because of the difference in reactivity between the two surfaces, (100) and (001), the monomers in the diffusion layer mainly flow into the (001) surface.

If the nanowires were formed via a diffusion-controlled lateral-growth mechanism,[12,13] they should grow in a relatively short period of time. However, 10 h appears to be too long for diffusion to be the rate-determining step. As shown in Figure 7b−d, a very small fraction of SrHAp nanowires with several micrometers in length began to form only after 1.5 h, and the number of wires increased with time without an increase in length. This phenomenon suggests that SrHAp nanowires were formed rather quickly but not during all the heating time. The several hours needed for a phase conversion may be due to the increase in the induction period, which is the time required for a critical supersaturation for dissolution to be reached.

III. Additional Discussion about the Shape Evolution. On the basis of the suggested arguments on the growth in a high or low pH solution, the bimodal distribution of the length of nanowires in the system produced at pH 10.3 (Figure 3) is understood to have originated from the coexistence of two phases, CS and SrHAp. The existing SrHAp experienced only intraparticle ripening (trimming), and CS changed into fractional SrHAp nanowires and TSP during heating at 180 °C. Consequently, a small fraction of SrHAp nanowires and many nanoparticles were produced simultaneously. As reported in the calcium-phosphate system by Bosky et al.,[49] existing hydroxyapatite did not act as a seed crystal for subsequent growth during transformations.

The supersaturation for the precipitation of SrHAp was also attained by mixing the source solution at pH 10.5 and 11.2 at 25 °C. However, the long-wire morphology was not observed under those conditions. This might be the result of the small driving force for phase conversion. The estimated driving forces for phase conversion at 25 °C with eqs 1, 2, and 10 in Appendixes II and III of the Supporting Information was only several kilojoules per mole, which was approximately 2 orders of magnitude lower than the driving forces at 180 °C. In the low chemical-potential environment, the dissolved monomers diffuse into all the surfaces and make a thermodynamically stable morphology (Figure 3).

There are many reports showing that nanowires/nanobelts with a high aspect ratio can be synthesized through the formation of amorphous precursor phases.[14,18,19] Since amorphous seeds experience dissolution and renucleation to crystalline particles during the hydrothermal process, it is possible that the amorphous prephase may play the role of a monomer injector, which stores the driving forces, releases them by dissolution, and creates the high chemical-potential environment needed for the one-dimensional growth during heating.

IV. Acquiring Strontium Hydroxyapatite Nanowires as a Major Phase. As mentioned in the above section, only a small fraction of the SrHAp nanowires had nucleated after 10 h of heating at 180 °C at a low pH (7.5 and 9.5). This is because the pH condition for SrHAp nucleation is not consistent with one-dimensional growth. Therefore, alternative methods are required to synthesize the SrHAp nanowires

(49) Boskey, A. L.; Posner, A. S. *J. Phys. Chem.* **1973**, *77*, 2313.

as a major phase. On the basis of the suggested mechanisms, the dried CS particles synthesized in the pH 7.5 solution were placed into a filtered clear solution from a suspension made in the initial pH 10.5 solution. Through this trial, a high chemical-potential environment for one-dimensional growth was artificially created in the high pH solution, where the SrHAp phase can be easily and rapidly formed.

The SrHAp nanowires were successfully synthesized with an appreciable proportion after only 10 h of heating at 180 °C, as shown in Figure 10a (despite the fractional TSP residual phase). Because of the complex entanglement of nanowires, the dried aggregates (in a centimeter scale) showed a texture like a fine filter-sheet morphology. In a recent report, the fine sheet was recommended as a matrix for the tissue engineering of bone and as a gene-delivery system.[50] In comparison, Figure 10b shows the morphology and phase obtained by mixing source solutions and heating the suspension only at pH 10.5 without any additional procedures. The experimental conditions used for the comparison were identical because the filtered solution from the pH 10.5 suspension was used as the solvent for the tactical trial. The clear difference in the two cases supports the suggested arguments on the function of the metastable precursor phase in synthesizing nanowires.

Conclusions

The nucleation and growth mechanisms of strontium hydroxyapatite were investigated, and nanowires with a high aspect ratio were synthesized by controlling the growth conditions. It was found that the least-stable CS phase precipitated in a low pH solution as a result of the slow sequential phase change, as predicted by the Ostwald rule of stages. In addition, only a small fraction of CS transformed to long SrHAp nanowires during heating at 180 °C. On the other hand, large-scale nanoparticles of the most-stable phase, SrHAp, with a low aspect ratio were easily synthesized after heating at a high pH.

The correlation between the precursor-phase constitution and the aspect ratio of SrHAp suggests that the anisotropic growth is promoted by the rapid release of stored chemical potential, through the dissolution of the metastable precursor particles (β-SHP or TSP at pH 7.5) and the renucleation of SrHAp. On the basis of this understanding, the optimum conditions for the nucleation of SrHAp and for the one-dimensional growth were determined, and considerable quantities of SrHAp nanowires were successfully acquired with an aspect ratio of several hundreds. This approach can be further extended to the convenient and high-volume synthesis of many types of nanowires with crystallographic anisotropy without the need for organic templates or surfactants.

Acknowledgment. The authors wish to acknowledge Ki-Bum Kim, Jaephil Cho, Joon-Gon Lee, Dongyeon Son, Hyun-Mi Kim, Kira Lee, and Sun-Young Kim for their helpful advice and materials characterization. This work was supported by the Basic Research Program (R01-2004-000-10173-0) of KOSEF, and the ERC program of MOST/KOSEF (R11-2002-102-00000-0).

Supporting Information Available: Effective reactions in the system and their solubility products at 25 and 180 °C, calculation of solubility isotherms as a function of pH, and the estimation of the driving forces for phase conversion from the metastable to the stable phase. This material is available free of charge via the Internet at http://pubs.acs.org.

IC051013M

(50) Ioku, K.; Yamauchi, S.; Fujimori, H.; Goto, S.; Yoshimura, M. *Solid State Ionics* **2002**, *151*, 147.